PAPER • OPEN ACCESS

Spin dynamics in helical molecules with nonlinear interactions

To cite this article: E Díaz *et al* 2018 *New J. Phys.* **20** 043055

New Journal of Physics
The open access journal at the forefront of physics

Deutsche Physikalische Gesellschaft DPG
IOP Institute of Physics

Published in partnership with: Deutsche Physikalische Gesellschaft and the Institute of Physics

OPEN ACCESS

RECEIVED
31 October 2017

REVISED
19 March 2018

ACCEPTED FOR PUBLICATION
4 April 2018

PUBLISHED
27 April 2018

PAPER

Spin dynamics in helical molecules with nonlinear interactions

E Díaz[1], P Albares[2], P G Estévez[2], J M Cerveró[2], C Gaul[1,3], E Diez[2] and F Domínguez-Adame[1]

[1] GISC, Departamento de Física de Materiales, Universidad Complutense, E-28040 Madrid, Spain
[2] NANOLAB, Departamento de Física Fundamental, Universidad de Salamanca, E-37008 Salamanca, Spain
[3] Cognitec Systems GmbH, Großenhainer Str. 101, D-01127 Dresden, Germany

E-mail: elenadg@ucm.es

Keywords: spin dynamics, chiral molecules, solitons

Abstract

It is widely admitted that the helical conformation of certain chiral molecules may induce a sizable spin selectivity observed in experiments. Spin selectivity arises as a result of the interplay between a helicity-induced spin–orbit coupling (SOC) and electric dipole fields in the molecule. From the theoretical point of view, different phenomena might affect the spin dynamics in helical molecules, such as quantum dephasing, dissipation and the role of metallic contacts. With a few exceptions, previous studies usually neglect the local deformation of the molecule about the carrier, but this assumption seems unrealistic to describe charge transport in molecular systems. We introduce an effective model describing the electron spin dynamics in a deformable helical molecule with weak SOC. We find that the electron–lattice interaction allows the formation of stable solitons such as bright solitons with well defined spin projection onto the molecule axis. We present a thorough study of these bright solitons and analyze their possible impact on the spin dynamics in deformable helical molecules.

1. Introduction

Manipulation and control of the electron spin degree of freedom in nanoscale materials lies at the very core of spintronics. Among the large variety of materials with technological interest in this field, organic systems are gaining significance as active components in spintronics nanodevices. Although large spin–orbit coupling (SOC) is uncommon in carbon-based materials, recent experiments on electron transport have brought with them a considerable effort to uncover the origin of the observed high spin selectivity in DNA [1, 2] and bacteriorhodopsin on non-magnetic metallic substrates [3]. As a working hypothesis, it has been suggested that spin selectivity may be related to the specific geometric structure of the involved molecular systems, namely their helical conformation [2]. A number of theoretical models have been put forward to explain the observed spin selectivity in helical molecules. Usually they rely on large SOC [4–12], the need for dephasing when SOC is weak [13, 14], the leakage of electrons from the molecule to the environment [15], the role of the bonding of the molecule to the metallic leads that enhance the effect [16, 17], or the interplay between a helicity-induced SOC and a strong dipole electric field, which is characteristic of these molecules [18] (see [19, 20] for a recent review). Theoretical models usually assume rigid lattices and neglect the local deformation of the molecule about the carrier. However, this assumption seems unrealistic to describe charge transport in molecular systems like DNA [21]. It is worth mentioning that theoretical models have taken into account the effects of molecular deformation only very recently [22, 23].

Depending on the various energy scales involved (electron bandwidth, zero-point energy of molecular vibrations, thermal energy), lattice deformation can play a significant role on transport properties. This is particularly relevant when charge carriers interact with intramolecular modes that occur at high frequency due to the stretching of stiff covalent bonds. Coupling to those modes may strongly alter charge transport [24] and even lead to self-trapping of carriers, provided that the relaxation energy (the energy gained upon the deformation of the lattice about the carrier) exceeds the bandwidth [25]. Self-trapping has been commonly

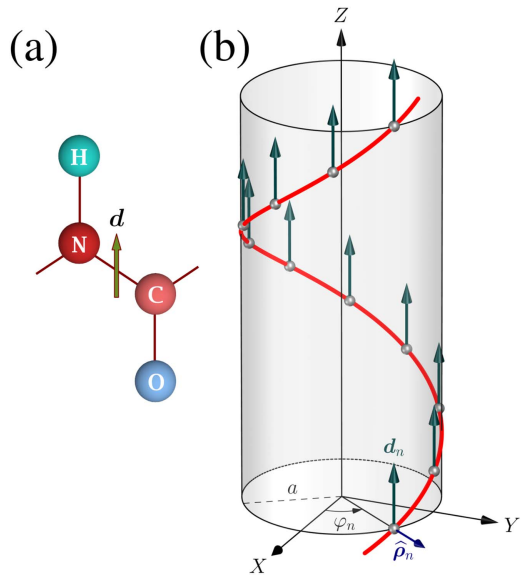

Figure 1. (a) Dipole moment of a peptide unit in an α-helix, according to Hol [35]. (b) Schematic view of the arrangement of the peptide dipoles $\boldsymbol{d}_n = d\hat{\boldsymbol{e}}_z$, aligned along the molecule axis. The dipoles shown here span a length along the Z axis equal to the molecule pitch b.

formulated within the framework of the small polaron theory based on a local Holstein-type coupling [26] between the carrier and the intramolecular mode. This model was later extended by Peyrard and Bishop to study the ac response of a DNA molecule, where the charge in the π-stack interacts with the base-pair opening dynamics of the double strand [27–30]. In a recent paper, Behnia *et al.* have studied the impact of the base-pair opening on the spin selectivity in DNA by using a generalization of the Peyrard–Bishop–Holstein [22].

Davydov's soliton theory of charge and energy transfer in α-helix and acetanilide provides another paradigmatic example on how the interaction of carriers and vibrational degrees of freedom can induce self-trapping phenomena [31]. Starting from a Frölich-like Hamiltonian [32] and assuming the adiabatic approximation, Davydov put forward a soliton theory of long-range energy transfer of excitations interacting with intramolecular vibrational modes in a quasi-one-dimensional lattice. In the adiabatic approximation, the continuous limit of the Davydov's equations reduce to the nonlinear Schrödinger (NLS) equation for the elementary excitations.

Inspired by the success of the Davydov's approach, in this work we introduce an effective self-focusing nonlinear model describing the dynamics of a single charge carrier in the electrostatic potential created by a helical arrangement of dipoles. The proposal generalizes the linear model formerly introduced by Gutiérrez *et al.* considering spin-selective transport of electrons through a helically shaped electrostatic potential [6]. This model has been recently revisited and extended to study the coherent spin dynamics in helical molecules [11]. The strong interaction with the lattice vibrations will be addressed by adding a nonlinear term to the Schrödinger equation within the adiabatic approximation [33]. The resulting equation turns out to be integrable, thus allowing us to obtain a family of bright solitons describing the coherent spin dynamics in deformable helical molecules.

2. Electron spin dynamics in a rigid helical molecule

Following [11], we start out by revisiting and amending the model introduced in [6]. Two main factors determine the high spin selectivity found: an unconventional Rashba-like SOC, reflecting the helical symmetry of molecules, and a weakly dispersive electronic band. α-helix in the secondary structure of proteins and other macromolecules present a net dipole moment along the helix axis due to the helical arrangement of peptide dipoles [34]. In an α-helix, the peptide dipoles are aligned in such a way that about 97% of the peptide dipole moments point in the direction of the helix axis [35] (see figure 1(a)). Therefore, α-helices can be regarded as macrodipoles, having a total dipole moment of the order of $3.5N$ Debye (N is the number of residues), pointing from the negative C-terminus to the positive N-terminus of the helix (see [36] and references therein). The magnitude of the electric dipole of the molecule is not a fixed value but depends on the molecular conformation and on its local environment. For instance, hydrogen bonds can yield a significant enhancement of the dipole moments, as pointed by Hol [35].

We thus consider the electron motion through a very long helical arrangement of peptide dipoles directed along the Z axis, as shown schematically in figure 1(b). The dipoles are located at $\boldsymbol{r}_n = n\Delta z\,\hat{\boldsymbol{e}}_z + a\,\hat{\boldsymbol{\rho}}_n$, a being the radius of the molecule, and their dipole moments are $\boldsymbol{d}_n = d\,\hat{\boldsymbol{e}}_z$. Here, we have used cylindrical coordinates with $\hat{\boldsymbol{\rho}}_n = (\cos\varphi_n,\ \sin\varphi_n,\ 0)$, and $\varphi_n = 2\pi\, n/N_d + \pi$, being N_d the number of dipoles per turn. The orientation of the individual dipoles does not affect much the results, provided they are arranged helically and parallel to each other [11].

The electric field generated by the dipoles aligned along the molecule axis reads

$$\boldsymbol{E}(\boldsymbol{r}) = \frac{1}{4\pi\epsilon_0}\sum_{n=-\infty}^{\infty}\left[3\,\frac{(\boldsymbol{r}-\boldsymbol{r}_n)\cdot\boldsymbol{d}_n}{|\boldsymbol{r}-\boldsymbol{r}_n|^5}\,(\boldsymbol{r}-\boldsymbol{r}_n) - \frac{\boldsymbol{d}_n}{|\boldsymbol{r}-\boldsymbol{r}_n|^3}\right]. \tag{1}$$

We will constrain the electron motion along the Z axis the position vector the is $\boldsymbol{r} = z\,\hat{\boldsymbol{e}}_z$. Thus, we get the following components of the electric field (1) in the XY plane

$$\begin{aligned} E_x(z) &= -\frac{3ad}{4\pi\epsilon_0}\sum_{n=-\infty}^{\infty}\frac{(z-n\Delta z)\cos\varphi_n}{[a^2+(z-n\,\Delta z)^2]^{5/2}},\\ E_y(z) &= -\frac{3ad}{4\pi\epsilon_0}\sum_{n=-\infty}^{\infty}\frac{(z-n\Delta z)\sin\varphi_n}{[a^2+(z-n\,\Delta z)^2]^{5/2}}. \end{aligned} \tag{2}$$

The transverse components of the electric field are needed to evaluate $\mathcal{E}(z) = -\mathrm{i}E_x(z) - E_y(z)$ (see [12] for further details). From equation (2) we obtain

$$\mathcal{E}(z) = -\mathrm{i}\,\frac{3ad}{4\pi\epsilon_0}\sum_{n=-\infty}^{\infty}\frac{(z-n\,\Delta z)\,\mathrm{e}^{-\mathrm{i}2\pi n/N_d}}{[a^2+(z-n\,\Delta z)^2]^{5/2}}. \tag{3}$$

For further estimations, notice that typical values are $N_d \sim 10$ dipoles per turn in DNA or $N_d \sim 5$ in α-helix. In the limit $N_d \gg 1$, equation (3) can be approximated by the formal substitution $\sum_n \to (b/\Delta z)\int \mathrm{d}u$, $u = (z - n\Delta z)/b$ being the dummy variable

$$\sum_{n=-\infty}^{\infty}\frac{(z-n\,\Delta z)\,\mathrm{e}^{-\mathrm{i}2\pi(z-n\Delta z)/b}}{[a^2+(z-n\,\Delta z)^2]^{5/2}} \simeq \frac{1}{b^3\Delta z}\int_{-\infty}^{\infty}\mathrm{d}u\,\frac{u\,\mathrm{e}^{\mathrm{i}2\pi u}}{(u^2+a^2/b^2)^{5/2}}. \tag{4}$$

After performing the integration we obtain the magnitude $\mathcal{E}(z)$ needed to calculate the SOC

$$\mathcal{E}(z) = \frac{2\pi d}{\epsilon_0\Delta z b^2}\,K_1(2\pi a/b)\,\mathrm{e}^{-\mathrm{i}2\pi z/b} \equiv \mathcal{E}_0\,\mathrm{e}^{-\mathrm{i}2\pi z/b}, \tag{5}$$

where K_1 is the modified Bessel function of the second kind.

The SOC Hamiltonian stems from the classical formula $\boldsymbol{\sigma}\cdot(\hat{\boldsymbol{p}}\times\boldsymbol{E})$, symmetrized such that the Hamiltonian is Hermitian. Here $\boldsymbol{\sigma}$ is a vector whose components are the Pauli matrices σ_x, σ_y, and σ_z. For $\hat{\boldsymbol{p}} = \hat{p}_z\,\hat{\boldsymbol{e}}_z$ the SOC Hamiltonian simplifies to

$$\widehat{H}_{\mathrm{SO}} = \frac{\lambda}{2}\left[\hat{p}_z\begin{pmatrix}0 & \mathcal{E}(z)\\ \mathcal{E}^*(z) & 0\end{pmatrix} + \begin{pmatrix}0 & \mathcal{E}(z)\\ \mathcal{E}^*(z) & 0\end{pmatrix}\hat{p}_z\right], \tag{6}$$

where $\lambda = \mathrm{e}\hbar/(2mc)^2$. The electron Hamiltonian $\widehat{\mathcal{H}} = \hat{p}_z^{\,2}/2m + \widehat{H}_{\mathrm{SO}}$ can be cast in the form $\widehat{\mathcal{H}} = E_b\widehat{H}$ where the dimensionless Hamiltonian $\widehat{H}$ reads

$$\widehat{H} = -\partial_\xi^2 - 2\pi\gamma\,\widehat{M}. \tag{7a}$$

Here we have defined $E_b = \hbar^2/2mb^2$, $\xi = z/b$, $\partial_\xi = \partial/\partial\xi$ and the dimensionless spin–orbit parameter $\gamma = \hbar\lambda\mathcal{E}_0/(2\pi bE_b)$. The matrix operator $\widehat{M}$ is given by

$$\widehat{M} = \begin{pmatrix}0 & \mathrm{e}^{-\mathrm{i}2\pi\xi}\\ \mathrm{e}^{\mathrm{i}2\pi\xi} & 0\end{pmatrix}\begin{pmatrix}\mathrm{i}\partial_\xi - \pi & 0\\ 0 & \mathrm{i}\partial_\xi + \pi\end{pmatrix}. \tag{7b}$$

The dimensionless Hamiltonian (7) is readily diagonalized since it commutes with the helical operator $\hat{q} = \hat{p}_z + \pi\sigma_z$. The corresponding normalized eigenfunctions and eigenenergies are

$$\boldsymbol{\chi}_{qs}(\xi) = \begin{pmatrix}\beta_\uparrow(s)\,\mathrm{e}^{\mathrm{i}(q-\pi)\xi}\\ \beta_\downarrow(s)\,\mathrm{e}^{\mathrm{i}(q+\pi)\xi}\end{pmatrix}, \qquad \varepsilon_{qs} = q^2 + \pi^2 - sq\alpha, \tag{8}$$

where $\alpha = 2\pi\sqrt{1+\gamma^2}$, $s = \pm 1$ and

$$\beta_\uparrow(s) = \frac{1}{2}\left[(1+s)\cos\phi + (1-s)\sin\phi\right],$$
$$\beta_\downarrow(s) = \frac{1}{2}\left[(1-s)\cos\phi - (1+s)\sin\phi\right], \tag{9}$$

satisfying $\beta_\uparrow^2(s) + \beta_\downarrow^2(s) = 1$, and

$$\tan\phi = \frac{\gamma}{1+\sqrt{1+\gamma^2}}. \tag{10}$$

Notice that the helical conformation of the electric dipoles gives rise to an the additional effective momentum $q_s = s\pi\sqrt{1+\gamma^2}$ even in the absence of SOC. Previous studies report on this fact as having an impact on the linear optical response as well [37].

Once the eigenvectors of the Hamiltonian (7*a*) have been obtained, we focus on the dynamics of an electron wave packet of the form

$$\boldsymbol{\chi}(\xi, t) = \sum_s \int_{-\infty}^{\infty} \frac{\mathrm{d}q}{2\pi}\, C_{qs}\boldsymbol{\chi}_{qs}(\xi)\, \mathrm{e}^{-\mathrm{i}\varepsilon_{qs}t}, \tag{11a}$$

where time is expressed in units of $\hbar/E_b$ and

$$C_{qs} = \int_{-\infty}^{\infty} \mathrm{d}\xi\, \boldsymbol{\chi}_{qs}^\dagger(\xi)\cdot\boldsymbol{\chi}(\xi, 0). \tag{11b}$$

Our magnitude of interest will be the time-dependent spin projection onto the molecule axis, also referred as helicity, which is calculated as follows

$$\mathrm{SP}(t) = \int_{-\infty}^{\infty} \mathrm{d}\xi\, \boldsymbol{\chi}^\dagger(\xi, t)\sigma_z\boldsymbol{\chi}(\xi, t) = \int_{-\infty}^{\infty} \frac{\mathrm{d}q}{2\pi}\left[(|C_{q,+1}|^2 - |C_{q,-1}|^2)\cos(2\phi)\right.$$
$$\left. + 2\sin(2\phi)\,\mathrm{Re}\left(C_{q,+1}^* C_{q,-1}\mathrm{e}^{\mathrm{i}(\varepsilon_{q,+1}-\varepsilon_{q,-1})t}\right)\right]. \tag{12}$$

Consider an initial wave packet with an arbitrary state of helicity $\boldsymbol{\chi}(\xi, 0) = f(\xi)[\cos(\theta)\boldsymbol{u}_\uparrow + \mathrm{e}^{\mathrm{i}\varphi}\sin(\theta)\boldsymbol{u}_\downarrow]$, where $f(\xi)$ is an arbitrary bell-shaped function of dimensionless width W. Here $\boldsymbol{u}_\sigma$ with $\sigma = \uparrow, \downarrow$ denotes an eigenvector of σ_z and the spin projection is defined by the angle θ. For the sake of concreteness we set $\varphi = 0$ and we refer to as *fully polarized* or *fully unpolarized* state when the spin is parallel to ($\theta = 0, \pi/2$) or out of ($\theta = \pi/4$, $3\pi/4$) the molecular axis. After a straightforward calculation one can obtain a closed expression for SP(t) that has a transient contribution which vanishes at large times $t \gg W\big/(4\pi\sqrt{1+\gamma^2})$. A transient time of $t \sim 40$ *fs* is roughly estimated for a highly localized initial state with $W \sim 1$ passing through a DNA molecule with a SOC parameter of the order of $\gamma \sim 0.1$. Thus, after a quick transient state, the spin projection reaches the asymptotic value given as $\mathrm{SP}_\infty = \mathrm{SP}(t \to \infty)$, where

$$\mathrm{SP}_\infty = \frac{1}{1+\gamma^2}\left[\cos(2\theta) - \gamma\sin(2\theta)\int_{-\infty}^{\infty}\mathrm{d}\xi\,|f(\xi)|^2\cos(2\pi\xi)\right]. \tag{13}$$

Notice that if we consider an initial *fully polarized* state with $\theta = 0$ ($\theta = \pi/2$) namely with spin parallel (antiparallel) to the molecule axis, the larger the SOC parameter, the smaller the asymptotic spin projection, as expected.

In experiments, however, an initially unpolarized current becomes spin polarized after being transmitted through the helical molecule. Therefore, our case of interest is an initial *fully unpolarized* wave packet with spin projection out of the molecule axis, i.e. along the X axis such as $\boldsymbol{\chi}(\xi, 0) = f(\xi)(-\boldsymbol{u}_\uparrow + \boldsymbol{u}_\downarrow)\big/\sqrt{2}$. Let us have a deeper look at this particular case, for which the coefficients (11*b*) read

$$C_{q,+1} = \frac{1}{\sqrt{2}}\left[\cos\phi\int_{-\infty}^{\infty}\mathrm{d}\xi\, f(\xi)\mathrm{e}^{-\mathrm{i}(q-\pi)\xi} - \sin\phi\int_{-\infty}^{\infty}\mathrm{d}\xi\, f(\xi)\mathrm{e}^{-\mathrm{i}(q+\pi)\xi}\right],$$
$$C_{q,-1} = \frac{1}{\sqrt{2}}\left[\sin\phi\int_{-\infty}^{\infty}\mathrm{d}\xi\, f(\xi)\mathrm{e}^{-\mathrm{i}(q-\pi)\xi} + \cos\phi\int_{-\infty}^{\infty}\mathrm{d}\xi\, f(\xi)\mathrm{e}^{-\mathrm{i}(q+\pi)\xi}\right], \tag{14}$$

which leads to the following expression for SP(t)

$$\mathrm{SP}(t) = -\frac{\sin(4\phi)}{2}\left\{\int_{-\infty}^{\infty}\mathrm{d}\xi\,|f(\xi)|^2\cos(2\pi\xi) - \mathrm{Re}\left[\mathrm{e}^{-\mathrm{i}\pi\alpha t}\int_{-\infty}^{\infty}\mathrm{d}\xi\, f(\xi)f^*(\xi+\alpha t)\mathrm{e}^{-\mathrm{i}2\pi\xi}\right]\right\}$$
$$+ \sin(2\phi)^2\sin(\pi\alpha t)\,\mathrm{Im}\left[\int_{-\infty}^{\infty}\mathrm{d}\xi\, f(\xi)f^*(\xi+\alpha t)\right]. \tag{15}$$

Notice that the last two integral involves the overlap of $f(\xi)$ and $f^*(\xi + \alpha t)$ and consequently vanish when $t \gg W/\alpha$. Therefore, at times larger than W/α the spin projection reaches a steady value, corresponding to the

time-independent term in equation (15). In this case, the asymptotic spin projection has a non-monotonous dependence on the magnitude of the SOC parameter and the time-independent integral approaches unity for a narrow wave packet. The asymptotic spin projection along the molecule axis becomes

$$|\mathrm{SP}_\infty| = \frac{\sin(4\phi)}{2} = \frac{\gamma}{1+\gamma^2}, \tag{16}$$

in agreement with Eq. (13). Therefore, the SOC rotates the electron spin and, after a quick transient, the spin projection along the molecule axis becomes nonzero.

3. Electron spin dynamics in a deformable helical molecule

In order to describe a deformable helical molecule where electron dynamics is affected by the lattice vibrations, we will assume that dipoles vibrate along the molecule axis independently of each other. The potential energy of an electron at position $\boldsymbol{r} = r\hat{\boldsymbol{e}}_z$ in the electric field created by the nth dipole is

$$V_n(z) = -\frac{ed}{4\pi\epsilon_0}\frac{z - z_n}{[a^2 + (z - z_n)^2]^{3/2}}, \tag{17}$$

where $z_n = n\Delta z + u_n$. After a Taylor expansion in the small displacement u_n from equilibrium and keeping up to the first order term, we get $V_n(z) \approx V_n^0(z) + \delta V_n(z)$. The potential energy $V_n^0(z)$ corresponds to the electron interaction with the dipole at equilibrium, as discussed in the previous section. The first order correction is given as

$$\delta V_n(z) = \frac{ed}{4\pi\epsilon_0 a^3} f\left(\frac{z - n\Delta z}{a}\right) u_n, \tag{18}$$

with $f(x) = (1 - 2x^2)/(1 + x^2)^{5/2}$. This function is sharply peaked at $x = 0$ and it can be replaced by a Dirac δ-function with the proper coupling constant (details will be given elsewhere). Therefore, the first order correction to the potential energy of the electron in the electric field created by the dipoles is

$$\delta V(z) = \sum_{n=-\infty}^{\infty} \delta V_n(z) = V_1 \sum_{n=-\infty}^{\infty} u_n \delta(z - n\Delta z), \tag{19}$$

V_1 being a positive constant. Following a lengthy but straightforward procedure introduced by Bang *et al.* [38], in the adiabatic limit it is found that $u_n = -C\boldsymbol{\chi}^\dagger(n\Delta z, t)\cdot\boldsymbol{\chi}(n\Delta z, t)$ with C a positive constant that depends on the mass of the dipole units and their frequency. We now proceed to the continuum limit and replace the summation in equation (19) by an integration

$$\delta V(z) = -V_1 C \int_{-\infty}^{\infty} \boldsymbol{\chi}^\dagger(\theta, t)\cdot\boldsymbol{\chi}(\theta, t)\delta(z - \theta), \tag{20}$$

and finally we get $\delta V(z) = -V_1 C\boldsymbol{\chi}^\dagger(z, t)\cdot\boldsymbol{\chi}(z, t)$. This energy is to be added to the Hamiltonian $\widehat{H}$ discussed in the previous section.

In this scenario, the dimensionless NLS describing the dynamics of the spinor state $\boldsymbol{\chi}(\xi, t)$ including the first order correction of the interaction due to the vibrating dipoles reads

$$\mathrm{i}\partial_t\boldsymbol{\chi}(\xi, t) = \widehat{H}\boldsymbol{\chi}(\xi, t) - 4g[\boldsymbol{\chi}^\dagger(\xi, t)\cdot\boldsymbol{\chi}(\xi, t)]\boldsymbol{\chi}(\xi, t), \tag{21}$$

where $\widehat{H}$ is given in equation (7*a*) and $g > 0$ is a dimensionless constant.

The integrability of this equation has been recently analyzed by using the Painlevé test [39] which requires that the components of $\boldsymbol{\chi}$ admit the Laurent expansion

$$\boldsymbol{\chi}(\xi, t) = \sum_{j=0}^{\infty}\begin{pmatrix} a_j(\xi, t)\,\phi(\xi, t)^{j-1} \\ b_j(\xi, t)\,\phi(\xi, t)^{j-1}\end{pmatrix}, \tag{22}$$

around the movable singularity manifold $\phi(x, t) = 0$. By means of this test, it can also be proved that equation (21) is the only integrable case of a model very recently put forward by Kartashov and Konotov to study the dynamics of Bose–Einstein condensates with helical SOC [40]. Furthermore, it reduces to the Manakov nonlinear system when the SOC vanishes [41, 42]. The well known singular manifold method [43] arises from the truncation of the Painleve series (22) and yields the following three component Lax pair for equation (21)

$$\partial_\xi \mathbf{\Psi} = \mathrm{i}\begin{pmatrix} -\mu & \Phi_1^* & \Phi_2^* \\ -\Phi_1 & \mu+\pi & -\pi\gamma \\ -\Phi_2 & -\pi\gamma & \mu-\pi \end{pmatrix}\mathbf{\Psi}$$

$$\partial_t \mathbf{\Psi} = \mathrm{i}\begin{pmatrix} \Phi_1\Phi_1^* + \Phi_2\Phi_2^* + 2\mu^2 & -\mathrm{i}\partial_\xi\Phi_1^* - 2\mu\Phi_1^* & -\mathrm{i}\partial_\xi\Phi_2^* - 2\mu\Phi_2^* \\ -\mathrm{i}\partial_\xi\Phi_1 + 2\mu\Phi_1 & -\Phi_1\Phi_1^* - 2\mu^2 & -\Phi_1\Phi_2^* \\ -\mathrm{i}\partial_\xi\Phi_2 + 2\mu\Phi_2 & -\Phi_2\Phi_1^* & -\Phi_2\Phi_2^* - 2\mu^2 \end{pmatrix}\mathbf{\Psi}$$
$$+ \mathrm{i}\pi\begin{pmatrix} -\pi(1+\gamma^2) & -\gamma\Phi_2^* + \Phi_1^* & -\gamma\Phi_1^* - \Phi_2^* \\ \gamma\Phi_2 - \Phi_1 & 0 & 0 \\ \gamma\Phi_1 + \Phi_2 & 0 & 0 \end{pmatrix}\mathbf{\Psi}, \tag{23}$$

where μ is the spectral parameter, $\mathbf{\Psi}$ is a three component eigenvector and, to avoid exponentials, we have defined the transformation

$$\boldsymbol{\chi}(\xi, t) = \frac{1}{\sqrt{2g}}\begin{pmatrix} \mathrm{e}^{-\mathrm{i}\pi(\xi+\pi t)}\,\Phi_1(\xi, t) \\ \mathrm{e}^{\mathrm{i}\pi(\xi-\pi t)}\,\Phi_2(\xi, t) \end{pmatrix}. \tag{24}$$

The singular manifold method has been applied in [39] to this Lax pair in order to derive Darboux transformations and an iterative procedure that yields solitonic solutions for equation (21).

For self-focusing nonlinear interaction ($g > 0$), it can be demonstrated that the following bright solitons (similar to the case of Davydov's soliton) are a solution to equation (21)

$$\boldsymbol{\chi}_s(\xi, t) = \sqrt{\frac{g}{2}}\,\mathrm{sech}\,[g(\xi + ct)]\,\mathrm{e}^{-\mathrm{i}\varphi_s(\xi,t)}\begin{pmatrix} \beta_\uparrow(s)\,\mathrm{e}^{-\mathrm{i}\pi\xi} \\ \beta_\downarrow(s)\,\mathrm{e}^{\mathrm{i}\pi\xi} \end{pmatrix}, \qquad s = \pm 1, \tag{25}$$

where $\beta_\uparrow(s)$ and $\beta_\downarrow(s)$ are given by (9). Here c is a free parameter representing the velocity of the soliton. The phase is defined as $\varphi_s(\xi, t) = [c/2 - s\pi\cos^{-1}(2\phi)]\xi + (c^2/4 - g^2 - \pi^2\gamma^2)t$. The existence of two different bright solitons due to the arbitrary choice of the constant $s = \pm 1$ is known as the Kramer doublet and it is directly related to the preservation of the time-reversal symmetry in the model. Notice that these solitons have a well defined helicity that depends on the SOC due to equation (10). Most importantly, this helicity is preserved along its propagation and it is found to be

$$|\mathrm{SP}_{\mathrm{sol}}| = |\beta_\uparrow^2(s) - \beta_\downarrow^2(s)| = \frac{1}{\sqrt{1+\gamma^2}}. \tag{26}$$

4. Connection with experiments

Having presented the salient features of solitons in deformable helical molecules, we now turn to discuss their relevance in experiments. In recent experiments on electron transport in organic helical molecules, it has been clearly demonstrated that an initially unpolarized current turns out to get highly polarized when passing through the molecule [1–3, 44–49]. Since the intrinsic SOC effects are rather weak in these molecules, theoretical models proposed to describe the experiments rely on SOC related to the peculiarities of the helical geometry. It is worth mentioning that all these models strongly depend on a phenomenological SOC which was roughly estimated to be $\alpha = 4$–12 meV nm [6]. It seems that this coupling, even in the best scenario, is not large enough to support the high degree of spin polarization observed in the experiments. All these approaches, however, neglected lattice deformations that strongly affect the electron dynamics in organic molecules.

In order to show the relevance of the nonlinear interaction between the lattice and the spin degree of freedom, figure 2 compares the spin projection achieved with the linear, SP_∞, and the nonlinear model, $\mathrm{SP}_{\mathrm{sol}}$, as given by equations (16) and (26) respectively. To understand the experimental situation when a spin unpolarized current is injected into the molecule, we will consider an initial localized wave packet with a spin projection such that $\theta = 3\pi/4$ (fully unpolarized in the sense discussed above). The wave packet evolves in time and, after a short transient time, it reaches a steady spin proyection given by equation (16), to be compared with that obtained for the stable soliton (26). Figure 2 clearly shows an outstanding result, namely, the nonlinearity strongly enhances the resulting spin projection of a coherent electron passing through a deformable helical molecule. Thus, lattice vibrations lead to a larger effective SOC in the molecule. We define the *enhancement factor* as $\eta = (|\mathrm{SP}_{\mathrm{sol}}| - |\mathrm{SP}_\infty|)/(|\mathrm{SP}_{\mathrm{sol}}| + |\mathrm{SP}_\infty|)$, as depicted in the inset of figure 2. This parameter assesses the effects of the lattice on the spin rotation capability of the deformable helical molecule. According to the curve shown in the inset of figure 2, the self-focusing nonlinear interaction has a major effect when the SOC is weak. And this is precisely the case of interest in experiments, as discussed below.

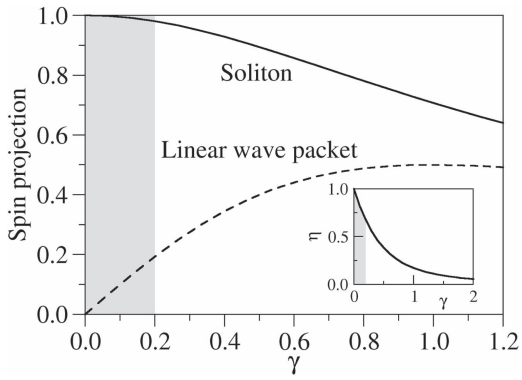

Figure 2. Asymptotic spin projection as a function of the dimensionless SOC parameter γ for a rigid helical molecule (dashed line) and a nonlinear deformable helical molecule (solid line). The inset shows the enhancement factor $\eta = (|\mathrm{SP_{sol}}| - |\mathrm{SP_{\infty}}|)/(|\mathrm{SP_{sol}}| + |\mathrm{SP_{\infty}}|)$. The gray area highlights the region with realistic values of γ according to to previous estimations [6].

The gray area of figure 2 highlights the region where the dimensionless SOC of our model takes values consistent with previous estimations $\gamma = \alpha/(2\pi b E_b) \leqslant 0.2$ in DNA. Our approach explains the physical scenario in experiments as follows. The initial unpolarized electron is injected in a deformable helical molecule whose vibrations interact continuously with the electronic dynamics inside the system. Such nonlinear interaction transforms the initial arbitrary state till it reaches the most stable configuration, namely, a solitonic solution. Once the soliton state is conformed, it can propagate with no dispersion along the molecule with a well defined high degree of helicity. The formation of solitons after a short transient time could be an important effect for the resulting highly polarized currents found in experiments.

5. Conclusions

In conclusion, we have presented a nonlinear model to study the spin dynamics of electrons in a deformable helical molecule. Such dynamics is subjected to: (i) the electric field created by the helical arrangement of molecular dipoles and (ii) the interaction between the electron and the lattice vibrations. On the one hand, the dipole electric field induces a Rashba-like SOC for electrons moving along the helical axis. On the other hand, the electron–lattice interaction allows the formation of stable solitons.

Once the model was presented, we were able to prove that the system supports the formation of stable bright solitons. Remarkably, the helicity of such solitons is preserved during the propagation across the helical molecule. We also calculated the spin projection onto the molecule axis as a figure of merit to assess the spin dynamics. For completeness, we also compared this result with those obtained for the linear model corresponding to the rigid molecule. In particular, we focused on the most relevant situation for experiments, namely the partial spin projection achieved by an initial unpolarized electron when passing through the helical molecule. In such scenario, the spin rotation capability of a deformable helical molecule is largely increased compared to the rigid one, even in the case of weak SOC.

Acknowledgments

The authors thank R Gutiérrez and V Mujica for helpful discussions. This research has been supported by MINECO (Grants MAT2013-46308 and MAT2016-75955) and Junta de Castilla y León (Grant SA045U16) and Junta de Castilla y León (Grant SA045U16) and P. Albares Ph.D. Fellowship.

ORCID iDs

E Diez https://orcid.org/0000-0001-7964-4148

References

[1] Göhler B, Hamelbeck V, Markus T Z, Kettner M, Hanne G F, Vager Z, Naaman R and Zacharias H 2011 *Science* **331** 894
[2] Xie Z, Markus T Z, Cohen S R, Vager Z, Gutiérrez R and Naaman R 2011 *Nano Lett.* **11** 4652
[3] Mishra D, Markus T Z, Naaman R, Kettner M, Gohler B, Zacharias H, Friedman N, Sheves M and Fontanesi C 2013 *Proc. Natl Acad. Sci. USA* **110** 14872

[4] Yeganeh S, Ratner M A, Medina E and Mujica V 2009 *J. Chem. Phys.* **131** 014707
[5] Medina E, López F, Ratner M A and Mujica V 2012 *Europhys. Lett.* **99** 17006
[6] Gutiérrez R, Díaz E, Naaman R and Cuniberti G 2012 *Phys. Rev.* B **85** 081404
[7] Eremko A A and Loktev V M 2013 *Phys. Rev.* B **88** 165409
[8] Rai D and Galperin M 2013 *J. Phys. Chem.* C **117** 13730–7
[9] Medina E, González-Arraga L A, Finkelstein-Shapiro D, Berche B and Mujica V 2015 *J. Chem. Phys.* **142** 194308
[10] Caetano R A 2016 *Sci. Rep.* **6** 23452
[11] Díaz E, Gutiérrez R, Gaul C, Cuniberti G and Domínguez-Adame F 2017 *AIMS Mater. Sci.* **4** 1052
[12] Gutierrez R, Díaz E, Gaul C, Brumme T, Domínguez-Adame F and Cuniberti G 2013 *J. Phys. Chem.* C **117** 22276
[13] Guo A M and Sun Q F 2012 *Phys. Rev. Lett.* **108** 218102
[14] Guo A M and Sun Q F 2014 *Proc. Natl Acad. Sci. USA* **111** 11658
[15] Matityahu S, Utsumi Y, Aharony A, Entin-Wohlman O and Balseiro C A 2016 *Phys. Rev.* B **93** 075407
[16] Guo A M, Díaz E, Gaul C, Gutierrez R, Domínguez-Adame F, Cuniberti G and Sun Q F 2014 *Phys. Rev.* B **89** 205434
[17] Wu H N, Wang X and Gong W J 2017 *Chem. Phys. Lett.* **677** 131
[18] Michaeli K and Naaman R 2015 arXiv:1512.03435
[19] Naaman R and Waldeck D H 2012 *J. Phys. Chem. Lett.* **3** 2178
[20] Michaeli K, Varade V, Naaman R and Waldeck D H 2017 *J. Phys.: Condens. Matter* **29** 103002
[21] Chakraborty T 2007 *Charge Migration in DNA: Perspectives from Physics, Chemistry, and Biology* (Berlin: Springer) (https://doi.org/10.1007/978-3-540-72494-0)
[22] Behnia S, Fathizadeh S and Akhshani A 2016 *J. Phys. Chem.* C **120** 2973
[23] Varela S, Mujica V and Medina E 2017 arXiv:1710.07204
[24] Nan G, Yang X, Wang L, Shuai Z and Zhao Y 2009 *Phys. Rev.* B **79** 115203
[25] Fratini S, Mayou D and Ciuchi S 2016 *Adv. Funct. Mater.* **26** 2292
[26] Holstein T 1959 *Ann. Phys.* **8** 325
[27] Peyrard M and Bishop A R 1989 *Phys. Rev. Lett.* **62** 2755
[28] Komineas S, Kalosakas G and Bishop A R 2002 *Phys. Rev.* E **65** 061905
[29] Maniadis P, Kalosakas G, Rasmussen K O and Bishop A R 2005 *Phys. Rev.* E **72** 021912
[30] Díaz E, Lima R P A and Domínguez-Adame F 2008 *Phys. Rev.* B **78** 134303
[31] Davydov A S 1979 *Phys. Scr.* **20** 387
[32] Fröhlich H 1954 *Adv. Phys.* **3** 325
[33] Datta P K and Kundu K 1996 *Phys. Rev.* B **53** 14929
[34] Sengupta D, Behera R N, Smith J C and Ullmann G M 2005 *Structure* **13** 849
[35] Hol W G J 1985 *Prog. Biophys. Mol. Biol.* **45** 149
[36] Adhya L, Mapder T and Adhya S 2013 *Biochim. Biophys. Acta* **1828** 845
[37] Díaz E, Malyshev A V and Domínguez-Adame F 2007 *Phys. Rev.* B **76** 205117
[38] Bang O, Christiansen P L, If F, Rasmussen K O and Gaididei Y B 1994 *Phys. Rev.* E **49** 4627
[39] Albares P, Díaz E, Cerveró J M, Domínguez-Adame F, Diez E and Estévez P G 2018 *Phys. Rev.* E **97** 022210
[40] Kartashov Y V and Konotop V V 2017 *Phys. Rev. Lett.* **118** 190401
[41] Manakov S V 1974 *Sov. Phys. -JETP* **38** 248 (www.jetp.ac.ru/cgi-bin/dn/e_038_02_0248.pdf)
[42] Vishnu Priya N, Senthilvelan M and Lakshmanan M 2013 *Phys. Rev.* E **88** 022918
[43] Estévez P G, Díaz E, Domínguez-Adame F, Cerveró J M and Diez E 2016 *Phys. Rev.* E **93** 062219
[44] Dor O B, Yochelis S, Mathew S P, Naaman R and Paltiel Y 2013 *Nat. Commun.* **4** 2256
[45] Kettner M *et al* 2015 *J. Phys. Chem.* C **119** 14542
[46] Mondal P C, Fontanesi C, Waldeck D H and Naaman R 2015 *ACS Nano* **9** 3377
[47] Einati H, Mishra D, Friedman N, Sheves M and Naaman R 2015 *Nano Lett.* **15** 1052
[48] Vankayala K, Mathew S P, Cohen S R, Hernández Delgado I, Lacour J and Naaman R 2016 *Adv. Mat.* **28** 1957
[49] Aragonés A C *et al* 2017 *Small* **13** 1613